TRAPPING LARGE WOOD DEBRIS IN RIVERS: EXPERIMENTAL STUDY ON A NOVEL DEBRIS RETENTION SYSTEM

Diego Panici[1] and Prakash Kripakaran[2]

[1]University of Exeter, North Park Road, Exeter, EX4 4QF, UK. Email: d.panici@exeter.ac.uk

[2]University of Exeter, North Park Road, Exeter, EX4 4QF, UK

ABSTRACT

Large wood debris can cause critical damage to bridges and other riverine structures, and increase flood risk. Although their effects on hydrodynamic actions and flood levels have been investigated in recent research, little effort has been devoted to reducing the amount of debris that can accumulate at structures. This paper proposes and experimentally tests a new type of large wood debris retention system in which a series of alternating porous and rack-type modules, is placed in-line with the current. Laboratory tests illustrate that the proposed retention system can offer high levels of efficiency in trapping large wood in rivers. The geometrical features of the structure are observed to play a major role and can be carefully chosen to optimise trapping efficiency. Results also show that large wood debris trapped by these structures have limited effects on the increase of the upstream water levels. Further development of the solution proposed in this work can pave the way for use of low-cost, highly-effective debris retention systems for effective river management and large wood debris removal in practice.

INTRODUCTION

Engineers face a major challenge in managing the consequences of the complex interactions between flow and structure for engineering works in rivers. Hydraulic structures (e.g. a bridge pier or abutment) in watercourses often cause obstructions to the flow that lead to a rise in the upstream water level, often referred to as afflux, which may increase the flood risk for adjacent areas. Localised scour is also likely to develop at such structures. This can undermine the foundations of structures and lead to significant structural damage and even collapse. Accumulations of large wood debris (also referred to as woody debris or debris in this manuscript), resulting from woody debris transported by rivers after recruiting them from their banks, can dramatically exacerbate the aforementioned effects of scour and afflux. For example, tree logs can become entrapped at in-channel structures such as bridge piers and then trap other large wood debris such as twigs and tree branches to form large accumulations (*Diehl*, 1997; *Lagasse et al.*, 2010; *Panici and de Almeida*, 2018). The size of these accumulations can be such that they obstruct a significant portion of the channel. Therefore these can have a noticeable effect on the flow around the structure, and particularly worsen afflux and scour. In fact, debris-induced scour remains one of the main causes of bridge failures in US, UK and Ireland (*Diehl*, 1997; *Benn*, 2013). For example, debris blockage was cited as the primary reason for the failure of the masonry arch bridge on the river Crane near Feltham (UK) in 2009 (*RAIB*, 2010). The blockage caused scour-induced subsidence of the abutments and resulted in closure of the bridge and the supported major railway line for many months. Another notable example is the large flooding event in Switzerland in 2005 that resulted in over 100 bridges being damaged by large wood debris (*Schmocker and Hager*, 2011).

Several experimental studies have investigated the formation of debris accumulations and their hydrodynamic effects. For example, *Bocchiola et al.* (2008) observed that the probability of logs being retained by a series of randomly distributed obstacles depends on flow velocity and log length. Similar observations were made by *De Cicco et al.* (2020). They showed that the initiation of a debris accumulation at a bridge pier depends significantly on the Froude number of the flow. Other studies considered the probability of large wood accumulating at bridge decks (*Schmocker and Hager*, 2011; *Gschnitzer et al.*, 2017) or at bridges with a single pier (*Gschnitzer et al.*, 2017; *Panici and de Almeida*, 2018, 2020a). For piers, the process of accumulation formation is known to involve three stages (*Panici and de Almeida*, 2018). Individual debris elements first get trapped at an hydraulic structure (e.g. a bridge pier); these elements then entrap further debris pieces until the accumulation reaches a maximum size that is dependent on the length of individual debris and the approach velocity of the flow; eventually, when the accumulation reaches a certain maximum size, the flow removes the accumulation and transports it downstream of the structure (*Panici and de Almeida*, 2018). Debris accumulations, by blocking a large portion of the flow area (*Schalko et al.*, 2019a), can significantly increase the afflux - by up to two times the undisturbed upstream flow depth in the worst cases. Several studies have also examined the scour effects of debris accumulations. *Ebrahimi et al.* (2018), using an experimental study, investigated the scour hole at a bridge pier for a large range of debris shapes and sizes and observed that the maximum scour depth in the presence of debris could be up to 3 times the depth without debris. Other experimental studies on the scour effects of debris (e.g. *Melville and Dongol*, 1992; *Lagasse et al.*, 2010; *Pagliara and Carnacina*, 2011) have also shown comparable results, although these differed in the debris shapes and sizes used.

Debris mitigation measures can offer a sensible, cost-effective approach for reducing the scour and flooding consequences for structures prone to debris accumulations. However there has been limited research to date on the use of such measures for the protection of riverine structures (especially bridge piers) beyond a few full-scale applications, mostly within the USA. For example, sweepers and hydrofoils have been employed to divert the debris from the upstream face of bridge piers (*Bradley et al.*, 2005), whereas fins and sacrificial piles have been used to accumulate debris away from the pier and hence reduce the size of the forming scour hole (*Bradley et al.*, 2005; *Lyn et al.*, 2003). *Franzetti et al.* (2010) also tested another solution - a ramp to accumulate debris upstream from a bridge pier. These measures, except in a few selective applications (e.g. *Franzetti et al.*, 2010), have not demonstrated satisfactory levels of performance in terms of protection offered to downstream structures from debris (*Bradley et al.*, 2005).

A potentially better solution than mitigation is the removal of floating debris from a river prior to it reaching the structure as this will eliminate the risks due to potential accumulations. Although the reintroduction of large wood in riverine environments may have positive effects to protection to fish habitat and micro-organism stabilisation (*Gregory et al.*, 1993; *Abbe and Montgomery*, 1996; *Lagasse et al.*, 2010), the risks and costs posed by debris to human lives, structures and networks (*Lassetre and Kondolf*, 2012) can be much larger and exceed the potential environmental benefits in many cases. Furthermore, trapped wood can be reintroduced back in rivers (*Thomas and Nisbet*, 2007) in a controlled manner, as is now common practice, for aquatic conservation as well as to improve channel stability and flood management (*Abbe and Montgomery*, 1996; *Gurnell et al.*, 2002). Few studies have provided useful insights into potential systems for debris retention and removal. *Lange and Bezzola* (2006) tested a series of horizontal racks, partly covering the width of the channel, for partial retention of transported debris; the racks in this study were perpendicular to the banks and did not consider the influence of the angle relative to the bank on trapping efficiency. *Lyn et al.* (2003) tested a deflector and a groin-like submerged structure to divert the large wood debris away from a bridge pier; results however showed limited benefits, with these structures even occasionally increasing the quantity of debris accumulating at the pier. Although *Bradley et al.* (2005) listed debris fins as potential effective measures to protect bridges from large wood debris, a recent study by *Schalko et al.* (2019b) showed that the probability of debris accumulating at a bridge was not affected. *Schalko et al.* (2019b) also tested bottom sills, that may offer a better performance than fins (e.g. a reduction up to 30% of accumulation probability) but strongly depend on flow conditions and sediment transport. *Schmocker and Weitbrecht* (2013) experimentally tested a debris retaining basin in a bend of a channel, where debris can be collected in flood conditions using their inertia to get them into the basin. However, this type of solution has some limitations. For example, the basin is functional only when the water level reaches a threshold value, while debris, on the other hand, may also be transported in much lower flow conditions. Furthermore, retention basins would require a large amount of available land, which may not be feasible for many rivers, for example in uplands and hilly environments.

In this paper, we propose an innovative type of debris retention system to protect riverine structures (e.g. bridge piers) from large wood debris accumulations. This system, which will be built upstream of a protected structure, is designed to trap a high percentage of floating debris while limiting costs for removal and remedial works and applicable to the broadest number of rivers and type of event, and having limited effects on the backwater. The system proposed includes a set of highly porous alternating rack-type modules where each module is placed such that it is in-line with the flow and extends partially across the river. The reason for the system only partially extending across the river is to avoid the following issues that are encountered when using regular full-width rack poles:

- Removal of logs can be difficult and costly, especially if access is limited from the banks (*Panici et al.*, 2020b);
- River navigation including for simple leisure activities may be impeded unless expensive and complex structures (e.g. gates, locks) are built;
- The increase in upstream water level is often significant (e.g. *Schmocker and Weitbrecht*, 2013; *Schalko et al.*, 2019a), which has considerable implications for flood risk.

We experimentally test the efficiency of this system in catching debris elements for a range of geometries and configurations of the modules, as well as for different flow and debris conditions. Results are used to understand the relationship between module parameters and efficiency, and thereby make recommendations on the design of the retention system. Findings will have implications for river management in practice and will pave the way for further developments in debris mitigation measures.

METHODOLOGY

The type of debris retention system proposed in this paper is shown in Figure 1. The system consists of a series of modules, each of which is an in-line structure designed such that it captures large wood debris with a desired level of efficiency while

- providing hydraulic continuity,

- having minimum impact on flow level increase, and
- offering ease of access for debris removal.

Each module has a width S and is placed transversely to the direction of the flow at an angle α (see Figure 1). At full-scale, each module may be realised using a series of intertwined poles that are driven in to the river bed. However this paper investigates only the hydrodynamic interactions between the system and the debris; the structural design and analysis of the modules are beyond the scope of this study.

Dimensional analysis

In order to provide similarity between model and prototype as well as to determine the main variables influencing the performance of the debris retention system, we performed a dimensional analysis. The following parameters related to the flow, debris and retention system are considered: the acceleration due to gravity g, the flow velocity v, the channel width T, the density of the fluid ρ, the dynamic viscosity of the fluid μ, the undisturbed water depth h, the length of a debris element L, the diameter of a debris element d, the stream-wise length of a module R, the width of a module S and the spacing between modules m. As described below, in our experiments the amount of trapped debris is found to grow approximately linearly with the amount of supplied debris. We therefore choose as dependent variable the efficiency e of the debris retention system. This efficiency (defined as the amount of debris pieces trapped by the structures divided by the total number of debris transported) is likely to be functionally dependent on the flow, debris and retention system parameters outlined previously. This dependency can be represented mathematically as follows:

$$e = f\,(v, \rho, \mu, h, g, L, d, R, S, m, T)\,. \tag{1}$$

Applying Buckingham's Π theorem, three repeating variables - i.e. S, v and ρ, have been selected from (1) to form 8 dimensionless groups:

$$e = f\left(\frac{\mu}{vS\rho}, \frac{h}{S}, \frac{gS}{v^2}, \frac{L}{S}, \frac{d}{S}, \frac{R}{S}, \frac{m}{S}, \frac{T}{S}\right). \qquad (2)$$

Some simplifications can be made to Equation (2).

- Replicating Reynolds similarity in the experiments is extremely difficult as the Reynolds number for prototype conditions is likely to be very large. Hence, assuming Reynolds number invariance, the corresponding term in (2) is ignored. Reynolds numbers for the experimental scenarios are however kept reasonably large, i.e. in the turbulent regime; this is an accepted practice and has been employed in similar experimental studies in past hydraulic research (e.g. *Wallerstein et al.*, 2001; *Bocchiola et al.*, 2008; *Panici and de Almeida*, 2018).
- Debris elements of different lengths but with equal diameter (on average) are used in the experiments, so that the ratio d/S can be neglected from (2). The inherent assumption is that debris diameter will have much smaller influence on the performance of the debris retention system than debris length. This assumption is supported by previous studies on debris-structure interactions at bridge piers (e.g. *Panici and de Almeida*, 2018) that have shown debris diameter to be of only secondary importance to debris entrapment and build-up processes. However, debris diameter may play a role in the porosity of the accumulation, which in turn may affect afflux; this aspect is not investigated in this paper.
- The spacing between the two modules that constitute the debris retention system is assumed to be sufficiently large to avoid interactions between individual debris elements; this would ensure that the performance of the system is not determined by the distance between subsequent modules. Hence, m/S can be removed from (2).
- The influence of the water depth on system efficiency e is assumed to be negligible since debris tends to float and accumulate at the free surface. In the experiments, therefore flow depth is kept sufficiently large to avoid interactions of debris with the channel bed.
- The Froude number relative to the characteristic length S, which is one of the dimensionless

groups, can be expressed instead with respect to L - i.e. as a debris Froude number $\mathsf{Fr_L}=v/\sqrt{gL}$; this is consistent with past studies on debris entrapment (*Bocchiola et al.*, 2008; *Panici and de Almeida*, 2018, 2020a).

Consequently, Equation 2 can be simplified as follows:

$$e = f\left(\frac{v}{\sqrt{gL}}, \frac{L}{S}, \frac{R}{S}, \frac{S}{T}\right). \tag{3}$$

(3) relates the efficiency of the debris retention system to the flow characteristics and the geometry describing the retention system. Therefore, the flume experiments (described in the next section) and the data analysis are designed to explore the influence of the dimensionless variables in (3) on the efficiency of the debris retention system.

Experiments

The experiments were conducted in a large, recirculating hydraulic flume at the University of Exeter. The prismatic flume is 14 m long, 0.61 m wide, and 0.70 m deep. Figure 1 shows sketches of the flume and the experimental setup adopted for this work as well as a photograph of the scale model of the retention system in the flume. The flume (glass-walled and with stainless steel bottom) was kept flat. Flow straighteners were present at its inlet to eliminate turbulence. The water depth was controlled using a flap gate at the downstream end of the flume. Discharge in the flume was varied between 0.042 m^3/s and 0.156 m^3/s, and was continuously monitored with a magnetic flow meter having a nominal accuracy of 0.5%. The water depth was measured at the flume centreline, 0.5 m upstream from the experimental area, using a digital point gauge (nominal accuracy of 0.05 mm) and it ranged between 0.209 m and 0.339 m. The average velocity at this section varied between 0.255 m/s and 0.763 m/s, and the Froude number ($\mathsf{Fr}=v/\sqrt{gh}$) ranged between 0.145 and 0.426, reflecting a wide range of Fr for floods in lowland and hilly rivers. Prior to each flow scenario, multiple measurements of the water depth across the experimental area were taken to ensure that differences in depth were minimal. This ensured a gradually varied flow with negligible convective accelerations.

The debris elements employed for these experiments were defoliated and non-branched natural sticks as recommended by past studies on debris (*Lyn et al.*, 2003; *Panici and de Almeida*, 2020a). Furthermore, natural sticks would display similar physical properties (e.g. density, elasticity) to large wood in rivers. The twigs used in this work were of two types: uniform and non-uniform in length, following the experiments by *Panici and de Almeida* (2018), to represent different types of debris in rivers. Scenarios with uniform length debris consisted of debris elements with the same length L. Experiments were run for two distinct values of L, namely L =0.25 m and L =0.175 m. On the other hand, scenarios with non-uniform debris used a mixture of debris elements with three lengths, namely L_1 =0.100 m, L_2 =0.175 m and L_3 =0.250 m, with each constituting the same proportion in the mixture. All debris elements had, on average, a diameter of 13.14 mm.

Four different types of debris retention systems were tested. These are referred to as experimental groups A, B, C, and D. Each system consisted of two modules: a primary module (i.e. the first module that debris would encounter) and a secondary module; both are shown in Figure 1. The modules are rectangular in shape with an aluminium frame on the outside. The inside of the rectangle is made up of a wire mesh - thin wires (0.25 mm) forming a square mesh of side 12.7 mm; the resulting porosity (i.e. the ratio between the void area and the area occupied by the modules) was always greater than 90%. The upstream tip of the first module was placed 7 m upstream from the flume outlet, and overall the system occupied the area between 5.3 m and 7 m from the outlet. The span-wise length S of the modules in groups A, B and C was kept equal to half-channel width - 0.305 m, or $S/T = 0.5$. However the streamwise length R of the modules is different for each group; this is to study the influence of the angle α (Figure 1), related to the dimensionless group R/S as α=arctan(R/S), on the efficiency of the system. α was 15°, 30° and 45° for groups A, B and C respectively with corresponding values for R being 0.082 m, 0.176 m and 0.305 m. Group D however differed from A, B and C. It had an angle α of 30°, but different values of S/T for the primary and secondary modules - namely $S/T = 0.25$ for the primary module, i.e. half the width S of the other modules, and $S/T = 0.50$ for the secondary module. In all the experimental groups, the modules were placed as shown in Figure 1, i.e. such that the primary module was mounted on the right bank and the secondary module from the left bank.

The performance of each of the retention systems, represented by the groups A, B, C and D, were evaluated using three debris scenarios as summarised in Table 1. The scenarios are identified using a numerical suffix alongside the group name of the retention system used in the experiment (e.g. A1, A2 and A3). Suffix 1 indicates scenarios run with debris having length $L = 0.25$ m; 2 indicates that scenarios run with $L = 0.175$ m; and 3 indicates scenarios that used debris elements of three different lengths in roughly equal proportion, i.e. $L_1 = 0.250$ m, $L_2 = 0.175$ m and $L_3 = 0.100$ m. Each debris scenario was studied for five different values of Fr_L, with two experimental runs conducted for each Fr_L value and the results averaged to compute system efficiency. The only exception is the system configuration with $\alpha = 30°$ (experimental groups B1-B3), for which tests were repeated four times for statistical robustness and to determine the standard deviation of the system efficiency. In total, 150 experiments were performed.

Experiments were carried out by dropping 100 sticks one-by-one in sequence at a cross-section 6 m upstream of the primary module. The number of debris elements was chosen based on two factors.

1. *Past research:* Past experimental studies (e.g. *Gschnitzer et al.*, 2017; *De Cicco et al.*, 2020) that have investigated the probability of formation of large wood debris accumulations at riverine structures have used between 50 and 100 debris elements.
2. *Field observations of large wood debris:* Several field surveys have noted that the total volume of water-borne wood during floods is typically between 100 and 1000 m^3 (*Ruiz-Villanueva et al.*, 2016; *Steeb et al.*, 2017), although values lower than 90 m^3 have also been observed in some instances (*Waldner et al.*, 2007; *Gschnitzer et al.*, 2017). A notable

example is the 2005 event in Switzerland in which wood volumes were observed for many rivers in the range 50 m^3 - 1000 m^3 (*Waldner et al.*, 2007; *Schmocker and Weitbrecht*, 2013; *Steeb et al.*, 2017). For the chosen experimental configuration, volumes of 90 and 1000 m^3 correspond to scaling factors of 30 and 66 respectively, for which the flume width would correspond to rivers having a channel width of 18 m and 40 m respectively.

The sticks were dropped at the flume centreline from a height of (approximately) 50 mm from the water surface. They were kept parallel to the flow direction and released at a frequency of approximately one element every 3 seconds. This frequency was selected to avoid interactions between individual elements, since previous research has shown that large wood debris move in rivers as individual elements rather than clusters (*Braudrick et al.*, 1997; *Diehl*, 1997; *Lyn et al.*, 2003, 2007; *Lagasse et al.*, 2010) although large masses of logs have also been occasionally observed, especially in mountainous areas (*Ruiz-Villanueva et al.*, 2019). A fixed camera placed 1 m upstream of the experimental area monitored continuously the entrapment of debris elements by the retention system. At the end of each test, the number of debris elements trapped at each module were counted. The number of debris elements that escaped the retention system and were captured at a wire mesh screen placed downstream of the flume were also counted. The water depth upstream of the modules was also measured at the beginning and at the end of each experiment to estimate the afflux caused by the accumulated debris. The depth was measured 0.50 m upstream from the most upstream tip of the first module, as shown in Figure 1, to allow sufficient room for the full development of the debris accumulation (i.e. the upstream extension of the accumulation from the first module was always less than 0.50 m). The afflux was measured as the ratio $\Delta h/h$, where h is the undisturbed flow depth and Δh is the increase in water depth, relative to h, at the end of the experiment.

RESULTS

Results from the experiments show common features upon collation. These are discussed in detail in the following sections.

General observations

The trapping of debris with time is analysed by using data from a set of 15 experiments involving groups C1, C2 and C3, covering all the tested $\mathsf{Fr_L}$ conditions. Figure 2 shows how the cumulative number of retained logs (vertical axis) varies with the total number of debris elements released (horizontal axis); the latter is proportional to time as the debris elements are released into the flume at a constant rate. The resulting relationship is essentially linear for all conditions with only minor variations (mostly due to individual elements passing through or being removed from the structures by impact with other incoming logs). The video footage of the same set of 15 experiments is also analysed to evaluate the variation in the number of logs trapped by individual modules of the retention system with time, and the results are shown in Figure 3. This figure, compared to Figure 2, however only shows data for three $\mathsf{Fr_L}$ conditions to ensure the plots are legible. Figure 3 shows that nearly equal number of debris elements are trapped by the two modules in the early stages of the experiments. However, this phenomenon is short-lived; the first module at low $\mathsf{Fr_L}$, (and, conversely the second module at high $\mathsf{Fr_L}$), traps a disproportionately larger number of debris with the progress of the experiment. These observations, based on Figures 2 and 3, are also true for the other experimental groups; the corresponding plots are not shown for reasons of brevity.

Image frames extracted from the footage of the experiments provide important insights in the process of accumulation of large wood debris at the trapping structures. Figure 4 shows four images (each for a different $\mathsf{Fr_L}$) of the debris accumulations at the modules for the experimental group C2 (chosen here as a representative example) at the end of each experiment. For low $\mathsf{Fr_L}$, the accumulation is in the form of a debris mat that extends into the upstream reach with most logs being retained at the first module, whilst only a small amount of large wood debris is trapped at the second module. However, increase in $\mathsf{Fr_L}$ gradually changes the size and geometry of the accumulated debris, and the distribution of logs between the two modules is also very different. There is a smaller number of logs at the first module and a larger number of logs at the second module. Also, the surface area of the accumulation has decreased while the vertical dimension (depthwise) of the accumulation has increased.

The analysis of video recordings can help understand the mechanism by which debris elements occasionally passed through the system. Figure 5 shows a sketch of the most commonly observed mechanism: the escaping elements reached the first module approximately at the centreline; then, after passing the first module, the elements followed the main flow lines (that on the surface were altered by the presence of the modules and accumulated debris) and, as a result, also passed by the second module. On a few occasions, these elements impacted the modules and then rotated about the outside frame of the rack. Other less frequent mechanisms involved oncoming logs impacting an accumulation and causing removal of one or a few debris elements. Analysis of the recordings show that all escaping elements follow a similar path after passing the second module. They are observed to be re-routed on the half-channel opposite to the second module. At larger Fr_L, the elements are seen to move further towards the far side of the flume, i.e. at high Fr_L most escaping elements are observed near the flume wall after the second module. This indicates that any obstacle (e.g. a bridge pier) in the downstream reach located away from this preferential path (i.e. away from the banks) is unlikely to interact with debris elements that may pass through the system.

Efficiency

The efficiency of the tested debris retention system is observed to be dependent on the debris Froude number Fr_L as well as on the type of debris employed. This is initially illustrated using results for groups B1 to B3 due to their relatively higher statistical robustness compared to those for other groups as a result of the larger number of experimental runs conducted for each value of Fr_L. Figure 6 shows on the vertical axis the percentage of debris (relative to the total number of debris elements released) trapped at the first and the second module as well as the percentage of debris that passed through the system for scenarios B1, B2 and B3 with respect to various values of Fr_L. Figure 6, using error bars, also displays the standard deviation in test results for groups B1-B3 for the four experimental runs conducted for each $\mathsf{Fr_L}$ value. It can be observed that the dispersion in results is typically small at high values of $\mathsf{Fr_L}$, while being significant at low $\mathsf{Fr_L}$. Furthermore, the levels of dispersion are generally similar for the three different debris scenarios, although, for L=0.175 m, a slightly smaller dispersion is visually discernible from the plots.

In general, better efficiency, between 85% and 92%, is observed for longer debris elements (group B1) compared to that for shorter debris elements (B2) or mixed debris (B3), for which the efficiency varies between 79% and 90% and between 72% and 81% respectively. Figure 6 also shows that, for low values of $\mathsf{Fr_L}$, the primary module traps a higher percentage of debris elements than the secondary module across all groups B1, B2 and B3. Nevertheless, for large values of $\mathsf{Fr_L}$, the trend is reversed; in these cases, the secondary module traps a higher percentage of debris elements with the primary module showing a markedly reduced ability to trap debris. While Figure 6 only shows results for one type of debris retention system (group B), the same tendency is also observed for the other systems.

Most experimental groups, i.e. configurations of the debris retention system, show a high debris entrapment efficiency. However, marked differences are observed between a few groups. Figure 7 shows the box plot of the debris retention efficiency for the four groups - A, B, C and D, for all flow conditions and debris types. The figure shows the average, upper and lower interquartiles and the total range of the efficiency of the various systems. Structures in groups C1 to C3 with $\alpha = 45°$ have the highest efficiency, which varies between 84% and 99% (92% on average) across all tested values of $\mathsf{Fr_L}$ and L. The efficiency decreases with decreasing α: for $\alpha = 30°$, i.e. groups B1 to B3, efficiency ranges between 74% and 97% (average 85%), whilst for $\alpha = 15°$, i.e. groups A1 to A3, efficiency ranges between 49% and 94% (average 70%). A different result is observed for group D in which the width of the first module is halved. The efficiency drops significantly; it ranges between 32% and 83% and has an average of 54%.

The efficiency results are now examined in relation to the size of debris elements. The observations are similar to those made for experimental group B from Figure 6. The size of debris elements do not have a notable influence on the system efficiency across all experimental groups, although a trend is evident. Figure 8 shows the efficiency versus $\mathsf{Fr_L}$ for all structures for different debris lengths L. The system is observed to have a high overall efficiency at the lowest range of $\mathsf{Fr_L}$ and the efficiency tends to decrease (or, conversely, the pass rate of debris elements increases) with increase in $\mathsf{Fr_L}$. Furthermore, the highest efficiency (e.g. 99% for C1 within group C) for an experimental group is generally observed for the longest debris elements (L=0.25 m) and this is especially true for low $\mathsf{Fr_L}$ values. Figure 9 shows the efficiency of the four tested structures for each tested debris length. For all structures except for structure type A, the efficiency is slightly lower for runs with shorter debris elements and runs with mixtures containing debris of different lengths. This trend is however less clear and definitive than for other variables (e.g. α) for structure types A, B and C; on the other hand, structure type D shows marked differences among groups D1, D2 and D3. Furthermore, the general trend of efficiency e decreasing with increasing $\mathsf{Fr_L}$ irrespective of the type of debris elements used, already observed in Figure 8, is also confirmed by the results given in Figure 9. A similar observation can also be made for the influence of the inclination of the retention system on efficiency; $\alpha = 45°$ shows the highest efficiency, with e reducing with decreasing α.

Afflux

The increase of the upstream water level (i.e. afflux) was also measured for each experiment. Figure 10 plots the afflux (calculated as the percentage increase in water level measured at the end of an experiment relative to the original undisturbed upstream water depth h) for the four tested structures versus $\mathsf{Fr_L}$ for the three debris scenarios. There is a clear trend of the afflux increasing with increase in $\mathsf{Fr_L}$. Nevertheless, the magnitude of the increase depends on the type of debris used: longer debris elements typically produce a larger increase in afflux than short elements or a mixture of debris having different lengths. For instance, the highest afflux (average of 11%), which is higher than that for short (B2) and mixed (B3) debris (average 7.8% and 7.4% respectively), is observed at $\mathsf{Fr_L}$≈0.41 for test B1 (α = 30°). The afflux is also dependent on the configuration of the retention system, i.e. the experimental group: the afflux is significantly higher for groups A and B (α = 15° and 30°) than for group C (α = 45°) - e.g. the maximum afflux for group C is 6.9%, below the maxima of 8.9% and 11.0% for groups A and B. For group D, the afflux is very low (maximum is 4.8%), although this can be explained by the generally low capacity of this structure to trap debris elements.

DISCUSSION

Efficiency

Experimental results clearly highlight the importance of the ratio S/T and the angle α. Group D, using modules with S/T =0.25, exhibits the least efficiency (Figure 7) amongst the tested groups. This result is according to expectation; the efficiency e is observed to drop with a decrease of the width of the module. These results also suggest that there may be potential to adjust S/T to obtain a desired efficiency; this may be useful to enable downstream transport of a certain level of large wood debris. Similar to the influence of S/T, the efficiency of the system is observed to rise with an increase in the angle α, with the best efficiency obtained for group C (Figure 7) with S/T = 0.5 and using the highest angle (α=45°) among the tested groups. While this finding may seem counter-intuitive, experimental observations revealed that, at small α values, the debris elements tended to rebound or be easily dislodged when they get entrapped near the edge of the modules. On the other hand, a sharper angle allowed debris to be dragged inward of the module toward the flume wall (i.e. the river bank at full-scale), effectively preventing debris elements from drifting away.

The influence of the log length on efficiency is less evident than that of α. Nevertheless, longer lengths are observed to lead to a higher trapping efficiency. This result, which aligns with findings from previous studies (*Bocchiola et al.*, 2008; *De Cicco et al.*, 2020) on debris accumulations, may be a consequence of the increased probability of interactions occurring between log and structure as well as amongst logs themselves, including interlocking. However, further research is required to accurately explain this behaviour. An important inference can also be made on the basis of the relationship between retention efficiency and wood volumes for the range tested in this study. The trend observed in Figure 2 highlighted that the amount of wood trapped by the system generally scales linearly with the amount of wood released. Therefore, the trapping efficiency can be expected to remain in the same observed range for the spectrum of volumes tested in this work.

Analysing the efficiency of the individual modules of the retention system over the duration of the experiments offers interesting insights. At the initial stages of each test, the proportion of trapped debris was roughly the same for the two modules, as shown visually for a few experimental runs in Figure 3. However, for low values of $\mathsf{Fr_L}$, as the accumulation at the first module extended into the opposite side of the channel (e.g., as observed in Figure 4a) its trapping capacity increased dramatically, resulting in most debris accumulating at the primary module and few elements being conveyed to the secondary module. Nevertheless, the exact opposite happens at high $\mathsf{Fr_L}$ values. In this case, elements at the edge of the first module were effectively removed by the flow and directed towards the second module, which was able to trap most of the debris elements. Therefore, the increase in $\mathsf{Fr_L}$ not only changed the physical conditions for which debris could accumulate at the two modules but also altered the size and geometry of the accumulation of logs (Figure 4). This behaviour is possibly due to the increase in drag force applied to the logs which then pulls the debris elements together and accumulates them under water.

Inferences can be drawn from the results on the need for a minimum of two modules within the proposed debris retention system. In the experiments, the two modules are spaced so that the efficiency of the primary module is independent of the presence of the secondary module (i.e. the secondary module's effects on flow do not extend up to the primary module). Consequently the results can be analysed to understand the efficiency of the primary module. Figure 6 shows the number of debris elements trapped by the primary and secondary modules in experimental group

B for various values of $\mathsf{Fr_L}$. The common trend amongst all experiments within group B (and also groups A and C) is that the trapping efficiency of the primary module decreases with $\mathsf{Fr_L}$; the exception is group D, i.e. for $S/T = 0.25$, for which the trapping efficiency tends to increase slightly with $\mathsf{Fr_L}$, although it remains extremely low compared to other cases. The results shown in Figure 6 reveal that a single module could be efficient at low values of $\mathsf{Fr_L}$. However, for large values of $\mathsf{Fr_L}$, a single module is likely to be inefficient; a second module would be required to trap the majority of debris elements.

Results enable comparing the performance of the proposed debris retention system with similar systems previously studied in literature. Table 2 shows a detailed analysis of these systems including standard debris racks. The table shows that group C1 ranks among the most efficient configurations. It demonstrates performance comparable to or better than *Schmocker and Weitbrecht* (2013). Only the structure proposed by *Hartlieb* (2017) performs better (i.e. 100%) than group C1, which may be a consequence of *Hartlieb*'s (2017) structure using a fine mesh and covering the complete channel width. Other measures either show a negative efficiency (e.g. *Lyn et al.*, 2003) or lower retention capacity (e.g. *Lange and Bezzola*, 2006).

Afflux

The afflux measurements provide useful insights on the potential flood risk impact of the employment of the proposed debris retention systems. The worst case for afflux are the scenarios with the highest $\mathsf{Fr_L}$ values, with the maximum afflux observed to be 11% of the water depth amongst all the tested scenarios. Nonetheless, the afflux is dependent on α; modules with α=45° would create the least afflux, and therefore minimise the increase in flood risk, whilst for α=15° and α=30° the afflux is more substantial, especially for higher $\mathsf{Fr_L}$. This result is potentially due to the accumulations causing a smaller reduction in the flow cross-section at α=45° because of the larger surface area (and consequently the larger volume) available for the debris to accumulate over relative to the other configurations.

The lowest levels of afflux are observed for Group D (Figure 10). This is likely because this group with an angle $\alpha = 30°$ has the lowest volume of accumulated wood of all the tested configurations. Similar results are also observed when the log lengths are different, as shown in Figure 10. The afflux for all four experimental groups was smaller for debris with length $L = 0.175$ m and debris of mixed lengths than for debris with length $L = 0.25$ m. The larger afflux was potentially due to the larger accumulation produced for $L = 0.25$ m than for the other two debris length scenarios.

Using Buckingham's Π theorem and making assumptions similar to those used for dimensional analysis of retention efficiency in the Methodology section, the increase in water depth arising from a debris accumulation at the proposed debris retention system can be defined by a functional relationship of the type:

$$\Delta h = f(h, V, S, R, \nu, g) \tag{4}$$

where V is the volume of accumulated debris. Therefore, together with the flow conditions, the increase in water depth Δh is caused by a relationship between the volume V of the debris accumulation and the maximum debris volume that each structure can hold as determined by the water depth h, and the size of the modules, i.e. S and R. This volume, which is denoted by V_C, is the volume of fluid enclosed by the two modules that can be occupied by the debris elements once they get trapped, i.e. for identical geometries of the two modules $V_C = hSR$. Thus, Equation (4) becomes:

$$\frac{\Delta h}{h} = f\left(\mathsf{Fr}, \frac{V}{V_C}\right). \tag{5}$$

A non-linear least-squares regression (with a bisquare weights method) on the afflux data given in Figure 10 was used to relate the non-dimensional parameters given in Equation (5) and resulted in the following function:

$$\frac{\Delta h}{h} = 5.01\mathsf{Fr}^{3.67}\left(\frac{V}{V_C}\right)^{0.50}. \tag{6}$$

For ease of representation on a 2D plane, if the product including Fr and V/V_C is defined as the accumulation factor $A_F = \mathsf{Fr}^{3.67}(V/V_C)^{0.50}$, Equation (6) becomes:

$$\frac{\Delta h}{h} = 5.01A_F. \tag{7}$$

Figure 11 shows the experimental data compared to the regression in Equation (7), with the afflux $\Delta h/h$ on the vertical axis and the accumulation factor A_F on the horizontal axis. The 95% prediction interval is also shown. The resulting regression from Equation (7) provided a regression coefficient $R^2 = 0.93$ and p-value $\ll 0.01$. Equation (7) and Figure 11 can facilitate afflux assessment for full-scale applications of the proposed retention system. In addition, since the volume of trapped large wood debris showed to accumulate linearly in time, up to the amount of volume V tested, it can be inferred that estimation of afflux through (7) is valid for the range of V/V_C tested.

Finally, the afflux for the proposed system is compared to those for debris retention structures tested in previous works (Table 2). The table shows that the system proposed in this paper causes minimal (i.e. up to 11%) increase in the upstream water level in contrast to full-width horizontal racks. For example, *Schalko et al.* (2019a) demonstrated that, depending on Fr and the wood packing density, backwater level can increase by up to 250% in conventional racks. Other systems (e.g. *Schmocker and Weitbrecht*, 2013) also typically doubled the upstream water level. Therefore the system proposed in this paper can offer superior performance in terms of afflux and consequential flood risks over other debris racks for the flow and wood variables tested.

Case study

In this section, the potential efficiency and effects of the four structures are evaluated for a real-world situation - a reach of the river Torridge in Devon, UK. Figure 12 shows the proposed location of the two modules and the first bridge structure that would be protected from large wood debris, namely Taddiport Bridge. Figure 12 also shows an accumulation of large wood debris that occurred at this bridge in 2012. The location chosen for this case study is in between Great Torrington and Taddiport. Downstream of this location, there are seven bridges known to be highly susceptible to large wood debris accumulations (*Panici et al.*, 2020b), with Old Rothern and Rothern (Rolle) bridges the worst affected. The area upstream of the considered location is not known to have flooding issues and an increase of backwater in the range observed in this study would not affect the risk of flooding. Also, the areas where the modules will be placed can be easily accessed from the banks for debris removal. The average channel width at the location in Figure 12 is 33.7 m, which corresponds to a model-prototype length scale factor of approximately 55. Table 3 shows the efficiency and afflux evaluated for the four different modules studied in the experiments. The performance of the retention system is assessed for six flood events (corresponding to different return periods) and for a large wood debris length of 13.8 m (corresponding to the model-scale length of 0.25 m). Assuming that 100 debris elements get transported during the events considered (consistent with the experimental conditions), the total equivalent volume of large wood debris at real-scale will equal 612 m^3. Such a volume is realistic; for example, a similar wood volume was observed at the river Emme in Switzerland in 2014 (*Ruiz-Villanueva et al.*, 2019).

The results shown in Table 3 highlight that flow conditions and wood characteristics (i.e. Fr and $\mathsf{Fr_L}$) are within the experimental range tested in this work for all return periods. Thus, the up-scaling can be performed to acceptable levels of accuracy. As revealed with the experimental data, the system efficiency varies according to the structure type. Type C (i.e. $\alpha = 45°$) provides the highest efficiency (96-99% of retained wood) and is also most robust, i.e. shows the smallest variation in efficiency across $\mathsf{Fr_L}$. In contrast, type A structure is less robust, with efficiency varying significantly across $\mathsf{Fr_L}$. The afflux increase is smallest for type B but only slightly worse for type C. Therefore, if the goal of the application of the retention system is to reduce as much as possible the amount of debris that can be transported downstream and at the same time limiting the afflux, the type C structure would provide the best performance.

Practical applications and future outlook

Using Froude similarity (and assuming that scale effects are negligible), results from this study can be up-scaled for full-scale scenarios. However, for scaling to be realistic, the values for flow and debris parameters including debris volume must be such that the computed dimensionless variables (e.g. Fr, $\mathsf{Fr_L}$) have values within the range studied in this paper. Considering the values of $\mathsf{Fr_L}$, Fr, and other variables tested in this work, results may be applicable mostly to hilly and/or lowland rivers. Practical issues may also need to be considered according to the structure that the system is designed to protect. For example, when applied to bridge piers in very wide rivers, the width of the racks may end up being significantly larger than the pier width, thus suggesting that other measures should be considered. Other aspects should also be accounted for when designing this structure: for example, the spacing between the mesh elements should be wide enough to minimise disturbance to the flow but also to avoid logs escaping through the gaps; the height of the modules should also exceed the water level of the design flood event plus any allowance for debris volume.

The retention system proposed in this paper may also be utilised to meet environmental requirements on river ecosystem continuity. The configuration of the racks enables removal of large wood debris from the banks during low flow. The removed debris can also be subsequently reintroduced at a downstream location. The system may instead also be designed to a certain efficiency to allow for a certain percentage of wood to be conveyed to the downstream reach of the river.

Further development of the proposed debris retention system requires consideration of other parameters that have been altogether excluded from or only partially investigated or in this work.

- Localised flow changes may have an effect on bank erosion: the flow components (especially on the surface) tend to display lateral components that may impact the stability of the channel banks. This would depend on the flow characteristics, the obstructed area and the condition of the channel banks (e.g. vegetation, soil).
- Large amounts of wood volume, moving *en masse* (also known as congested or hyper-

congested transport), were not tested in this study. Practical applications in which this situation is expected - e.g. mountainous rivers in which wood transport can be very high (*Ruiz-Villanueva et al.*, 2019), may result in inaccurate estimations.

- Finally, localised scour should be considered, since a likely configuration in full-scale would include poles embedded into the river bed. Nonetheless, these poles are likely to be typically small in width and pose minimal obstruction to the flow by themselves; hence, the resulting scour depth due to the racks themselves is expected to be manageable. However, accumulated large wood debris is likely to result in scour and this needs to be evaluated and accounted for in the design and operation of the retention system. Measures should also be considered to allow continuity of bed-load sediment transport by, for example, limiting the blockage at bed level. Moreover, accumulated large wood debris may change sediment transport rates at the racks depending on the debris blockage area.

CONCLUSIONS

In this paper, we proposed a large wood debris retention system for use in rivers for bridge protection and effective management of debris mitigation measures, and experimentally tested its efficiency using scale models. The system consists of two modules, which were designed as meshed racks placed from the side to the middle of the channel and with an inclination relative to the flow direction. The experiments were aimed at evaluating how the debris trapping efficiency of the system was influenced by the geometrical properties of the modules and the flow and debris parameters.

Experimental results support the following conclusions.

- The angle α between the system and the flow direction has a major influence on the system efficiency. The efficiency is maximum for α=45° for all the flow conditions and types of debris used and decreases with decreasing values of α.
- Highest efficiency is reached when the ratio *S*/*T* is equal to 0.50, i.e. the width of the structure is greater or equal than the channel width. The use of systems with smaller widths

resulted in a significantly smaller overall efficiency.

- A dual-module layout was crucial for the high efficiency achieved in the tests. At low $\mathsf{Fr_L}$ values, most of the debris are trapped by the primary module. As $\mathsf{Fr_L}$ increases the contribution of the secondary module to overall efficiency increases while that of the primary module reduces.
- The system has a relatively low impact on upstream afflux. For the case of α=45°, the water level increase ranged between 0.5% and 10%. Other tested values of α produced slightly higher values of afflux.

The systems tested in this paper represent the first evaluation of a novel concept of a debris retention system. Compared to regular full-width debris racks, the concept proposed in this paper has (i) a high retention efficiency (equal or similar to full-width racks) and (ii) causes limited increase in backwater levels (and thus flood risk) compared to the very high increases (up to 300%) observed with other solutions. The system also provides continuity for navigation as well as reduced costs, both constructional and operational. The former, since it would not occupy large areas or require construction of further structures (e.g. a gate); the latter, since it would require low maintenance and the removal of logs can be carried out from the banks, minimising or avoiding the costs for use of heavy machinery and impacts on traffic if removing debris from within the river. Further research is required in order to better understand structural design and its practical application at full scale. Its application at full scale might be expected to significantly reduce the amount of debris conveyed along a river and to provide bridge owners or overseeing organisations an easier and more cost-effective way to remove and relocate large wood debris in rivers.

DATA AVAILABILITY STATEMENT

Some or all data, models, or code generated or used during the study are available in a repository online in accordance with funder data retention policies. Data supporting the results presented in this paper are openly available from the University of Exeter repository at doi: http://doi.org/...

ACKNOWLEDGEMENTS

The authors received financial support for this research by the UK Engineering and Physical Sciences Research Council (EPSRC) through an Impact Acceleration Award, grant number EP/R511699/1. The authors are also grateful to the Devon County Council (UK) for the financial and material support provided for this research. The authors would like to thank Mr Julian Yates for the material help with the flume and experimental set-up. The authors are also grateful to the anonymous reviewers for their comments which improved substantially the quality of this manuscript.

REFERENCES

Abbe, T.B., and D. Montgomery (1996), Large woody debris jams, channel hydraulics and habitat formation in large rivers, *Regulated Rivers*, *12*, 201–221.

Benn, J. (2013), Railway bridge failure during flooding in the UK and Ireland, *Proceedings of the Institution of Civil Engineers*, *166*(4), 163–170.

Bocchiola, D., M.C. Rulli, and R. Rosso (2008), A flume experiment on the formation of wood jams in rivers, *Water Resources Research*, *44*(2), https://doi.org/10.1029/2006WR005846.

Bradley, J.B., D.L. Richards, and C.D. Bahner (2005), Debris control structures - evaluation and countermeasures, Federal Highway Administration, U.S. Department of Transportation, Washington D.C., USA.

Braudrick, C.A., G.E. Grant, Y. Ishikawa, and H. Ikeda (1997), Dynamics of wood transport in streams: A flume experiment, *Earth Surface Processes and Landforms*, *22*, 669–683.

De Cicco, P.N., E. Paris, L. Solari, and V. Ruiz-Villanueva (2020), Bridge pier shape influence on wood accumulation: Outcomes from flume experiments and numerical modelling, *Journal of Flood Risk Management*, DOI: 10.1111/jfr3.12599.

Diehl, T.H. (1997), Potential drift accumulation at bridges, Federal Highway Administration, U.S. Department of Transportation, Washington D.C., USA.

Ebrahimi, M., P. Kripakaran, D. Prodanovic, R. Kahraman, M. Riella, G. Tabor, S. Arthur, and S. Djordević (2018), Experimental study on scour at a sharp-nose bridge pier with debris blockage, *Journal of Hydraulic Engineering*, *144*.

Franzetti, S., and A. Radice, and M. Rabitti, and G. Rossi (2010), Hydraulic Design and Preliminary Performance Evaluation of Countermeasure against Debris Accumulation and Resulting Local Pier Scour on River Po in Italy, *Journal of Hydraulic Engineering*, *137*.

Gregory, K., R. Davis, and S. Tooth (1993), Spatial distribution of coarse woody debris dams in the Lymington Basin, Hampshire, UK, *Geomorphology*, *6*, 207–224.

Gschnitzer, T., and B. Gems, and B. Mazzorana, and M. Aufleger (2017), Towards a robust assessment of bridge clogging processes in flood risk management, *Geomorphology*, *279*, 128–140.

Gurnell, A.M., and H. Piégay, and F. Swanson, and S. Gregory (2002), Large wood and fluvial processes, *Freshwater Biology*, *47*, 601–619.

Hartlieb, A. (2017), Decisive Parameters for Backwater Effects Caused by Floating Debris Jams, *Open Journal of Fluid Dynamics*, *7*, 475–484.

Lagasse, P., P. Colopper, L. Zevenbergen, W. Spitz, and L. Girard (2010), Effects of debris on bridge pier scour, National Cooperative Highway Research Program, Transportation Research Board, Washington D.C., USA.

Lange, D., and G.R. Bezzola (2006), Schwemmholz: Probleme und Lösungsansätze (Large wood: Problems and solutions). VAW-Report 188, H.-E. Minor, ed. ETH Zurich.

Lassetre, N.S., and G.M. Kondolf (2012), Large woody debris in urban stream channels: redefining the problem, *River Research and Applications*, *28*, 1477–1487.

Lyn, D., T. Cooper, Y. Yi, R. Sinha, and A. Rao (2003), Debris accumulation at bridge crossing:

Laboratory and field studies, Federal Highway Administration, U.S. Department of Transportation, Washington D.C., USA.

Lyn, D., T. Cooper, C. Condon, and G. Gan (2007), Factors in Debris Accumulation at Bridge Piers, Federal Highway Administration, U.S. Department of Transportation, Washington D.C., USA.

Melville, B.W., and D. Dongol (1992), Bridge pier scour with debris accumulation, *Journal of Hydraulic Engineering*, *118*, 1306–1310.

Pagliara, S., and I. Carnacina (2011), Influence of wood debris accumulation on bridge pier scour, *Journal of Hydraulic Engineering*, *137*, 254–261.

Panici, D., and G.A.M. de Almeida (2018), Formation, growth, and failure of debris jams at bridge piers, *Water Resources Research*, *54*, https://doi.org/10.1029/2017WR022177.

Panici, D., and G.A.M. de Almeida (2020), Importance of pier geometry and debris characteristics on woody debris accumulations at bridge piers, *Journal of Hydraulic Engineering*, *145*, DOI: 10.1061/(ASCE)HY.1943-7900.0001757.

Panici, D., P. Kripakaran, S. Djordjević, and K. Dentith (2020), A practical method to assess risks from large wood debris accumulations at bridge piers, *Science of the Total Environment*, *728*, DOI: 10.1016/j.scitotenv.2020.138575.

Parola, A.C., C.J. Apelt, and M.A. Jempson (2000), Debris Forces on Highway Bridges, National Cooperative Highway Research Program, Transportation Research Board, Washington D.C., USA.

RAIB (Rail Accident Investigation Branch) (2010), Failure of Bridge RDG1 48 (River Crane) Between Whitton and Feltham 14 November 2009, Department for Transport, Derby, UK.

Ruiz-Villanueva, V., H Piégay, A.M. Gurnell, R.A. Marston, and M. Stoffel (2016), Recent advances quantifying the large wood dynamics in river basins: New methods and remaining challenges, *Review of Geophysics*, DOI: 10.1002/2015RG000514.

Ruiz-Villanueva, V., B Mazzorana, E. Bladé, L. Bürkli, P. Iribarren-Anacona, L. Mao, F. Nakamura, D. Ravazzolo, D. Rickenmann, M. Sanz-Ramos, M. Stoffel, and E. Wohl (2019), Characterization of wood-laden flows in rivers, *Earth surface processes and landforms*, *44*, 1694–1709, DOI: 10.1002/esp.4603.

Schmocker, L., and W.H. Hager (2011), Probability of Drift Blockage at Bridge Decks, *Journal of Hydraulic Engineering*, *137*, 470–479.

Schmocker, L., and V. Weitbrecht (2013), Driftwood: Risk Analysis and Engineering Measures, *Journal of Hydraulic Engineering*, *139*, 683–695.

Schalko, I., L. Schmocker, V. Weitbrecht, and R.M. Boes (2019a), Laboratory Flume Experiments on the Formation of Spanwise Large Wood Accumulations: I. Effect on Backwater Rise, *Water Resources Research*, *55*, 4854–4870.

Schalko, I., L. Schmocker, V. Weitbrecht, and R.M. Boes (2019b), Risk reduction measures of large wood accumulations at bridges, *Environmental Fluid Mechanics*, *20*, 485–502.

Steeb, N., D. Rickenmann, A. Badoux, C. Rickli, and P. Waldner (2017), Large wood recruitment processes and transported volumes in Swiss mountain streams during the extreme flood of August 2005, *Geomorphology*, *279*, 112-127, DOI: 10.1016/j.geomorph.2016.10.011.

Thomas, H., and T. Nisbet (2007), Modelling the hydraulic impact of reintroducing large woody debris into watercourses, *Journal of Flood Risk Management*, *5*, 164–174.

Wallerstein, D., and C.V. Alonso (2001), Distorted Froude-scaled flume analysis of large woody debris, *Earth Surface Processes and Landforms*, *26*, 1265–1283.

Waldner, P., C. Rickli, D. Köchlin, T. Usbeck, L. Schmocker, and F. Sutter (2007), Schwemmholz. Ereignisanalyse Hochwasser 2005 – Teil 1: Prozes se, Schäden und erste Einordnung (in German). Bundesamt für Umwelt BAFU, Eidgenössische Fors chungsanstalt, in UmweltWissen, vol. 0825, edited by W.S.L.G.R. Bezzola and C. Hegg, pp. 181–193, Bundesamt für Umwelt BAFU, Bern, Switzerland.

List of Tables

TABLE 1. Summary of experimental tests conducted in this work

Group	S/T	L/S	α	Flow depth range (mm)	Fr range
A1	0.50	0.82	15	248 - 318	0.143 - 0.426
A2	0.50	0.57	15	248 - 318	0.143 - 0.426
A3	0.50	0.57*	15	248 - 318	0.143 - 0.426
B1	0.50	0.82	30	209 - 275	0.143 - 0.418
B2	0.50	0.57	30	209 - 275	0.143 - 0.418
B3	0.50	0.57*	30	209 - 275	0.143 - 0.418
C1	0.50	0.82	45	317 - 335	0.145 - 0.421
C2	0.50	0.57	45	317 - 335	0.145 - 0.421
C3	0.50	0.57*	45	317 - 335	0.145 - 0.421
D1	0.25**	0.82	30	314 - 339	0.147 - 0.414
D2	0.25**	0.57	30	314 - 339	0.147 - 0.414
D3	0.25**	0.57*	30	314 - 339	0.147 - 0.414

*average length of debris mixture
**only for the first module

TABLE 2. Comparison among experimental results on debris retention structures

Study	Rack characteristics	Retention efficiency	Afflux range ($\Delta h/h$)
Lyn et al. (2003)	Submerged groin-like structure to deflect the flow	Smaller than without structure	N/A
Lyn et al. (2003)	Single pile deflector	Smaller than without structure	N/A
Lange and Bezzola (2006)	Horizontal racks in alternate order placed across the channel (steep-gradient rivers)	42-87% (27-35% if excluding deposition on river bed)	N/A
Schmocker and Weitbrecht (2013)	Bypass retention basin	90-95%	100-170%
Hartlieb (2017)	Retention racks at spillways	100%	5-45%
Schalko et al. (2019a)	Accumulated large wood debris at a rack with fixed and mobile bed	N/A	0-250%
This work	Alternate racks spanning half-channel and at an angle to the flow	Depending on α and S/T, between 91-99% (group C1) and 32-64% (group D2)	Depending on α and S/T, between 0-3.8% (group D2) and 0-11% (group B1)

TABLE 3. Application to a case-study on the river Torridge in Devon (UK): Estimation of efficiency and afflux for flood events with return periods of 2, 5, 10, 25, 100 and 200 years.

Quantity	**Flood event return period**					
	2	**5**	**10**	**25**	**100**	**200**
Discharge (m^3s^{-1})	250	327	385	472	638	743
Froude number Fr	0.343	0.348	0.352	0.357	0.365	0.369
Debris Froude number Fr_L	0.164	0.182	0.195	0.211	0.238	0.253
Efficiency *e* (group A) (%)	88	86	85	83	80	78
Efficiency *e* (group B) (%)	91	92	92	92	91	90
Efficiency *e* (group C) (%)	99	98	98	97	96	96
Efficiency *e* (group D) (%)	83	82	81	80	78	78
Afflux $\Delta h/h$ - group A (%)	14.9	14.2	13.9	13.5	13.1	12.8
Afflux $\Delta h/h$ - group B (%)	10.3	10.0	9.86	9.70	9.48	9.37
Afflux $\Delta h/h$ - group C (%)	10.5	10.5	10.6	10.6	10.8	10.9
Afflux $\Delta h/h$ - group D (%)	12.4	11.97	11.71	11.5	11.1	11.0

List of Figures

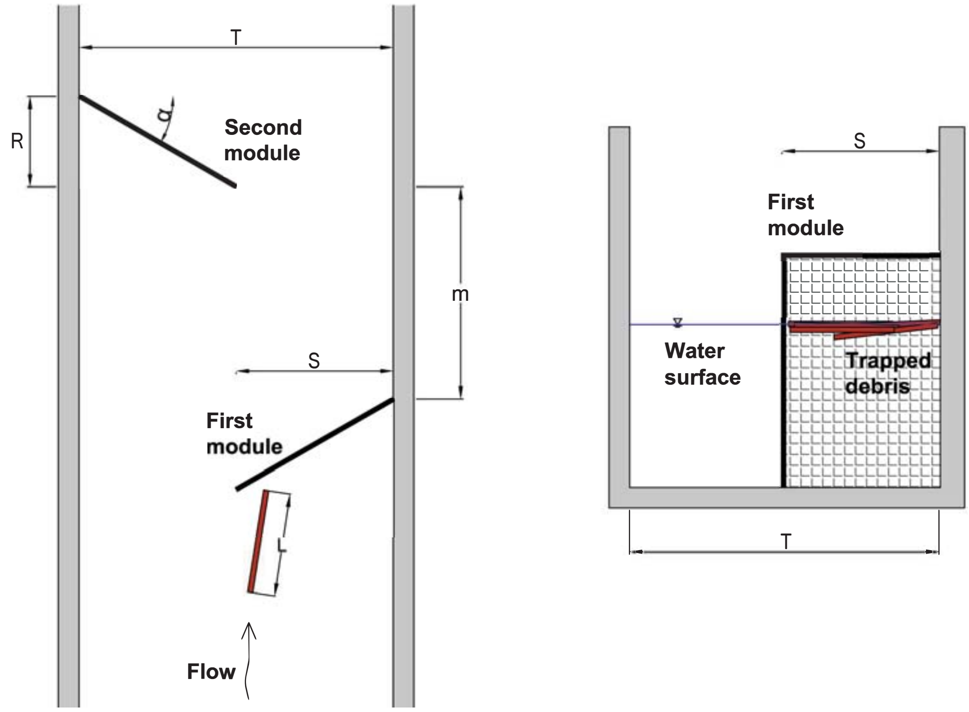

(a)

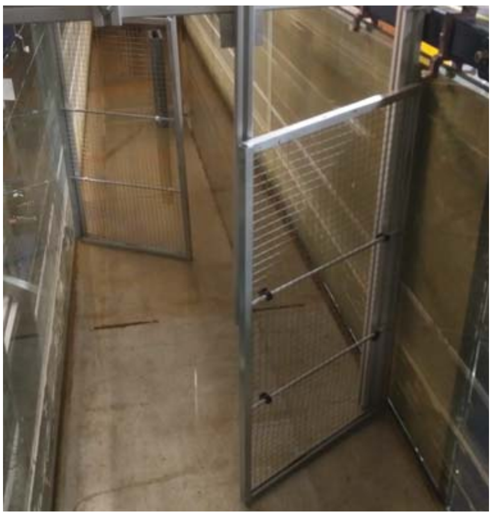

(b)

Fig. 1. Plan view (left) and cross-section view (right) of the flume and experimental set-up showing relevant variables (1a) and a downstream view of the experimental apparatus employed in this work (1b)

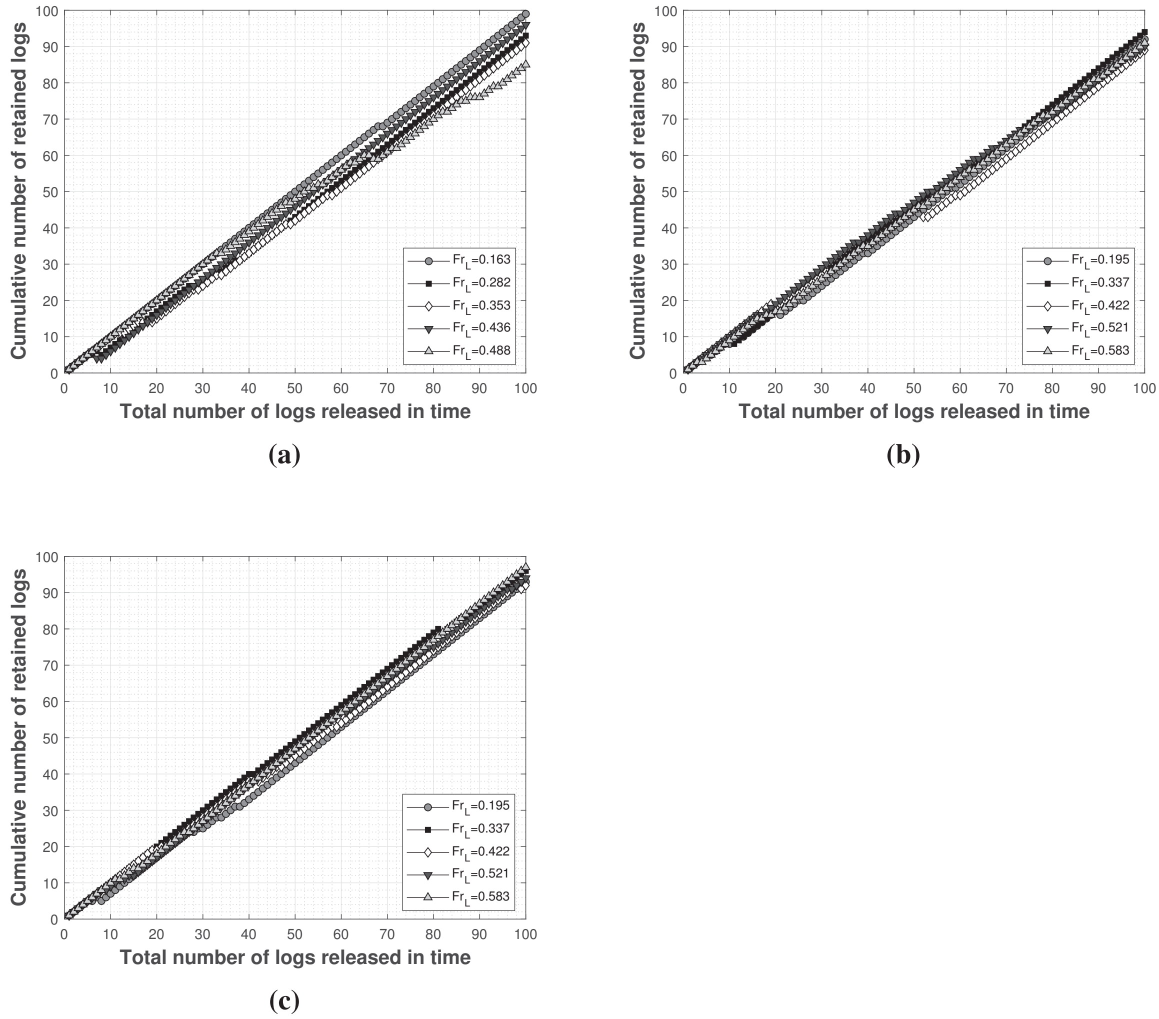

Fig. 2. Cumulative number of large wood debris trapped by the retention system (vertical axis) versus the number of debris released in time (horizontal axis) for groups C1 (2a), C2 (2b) and C3 (2c) for the range of tested Fr_L.

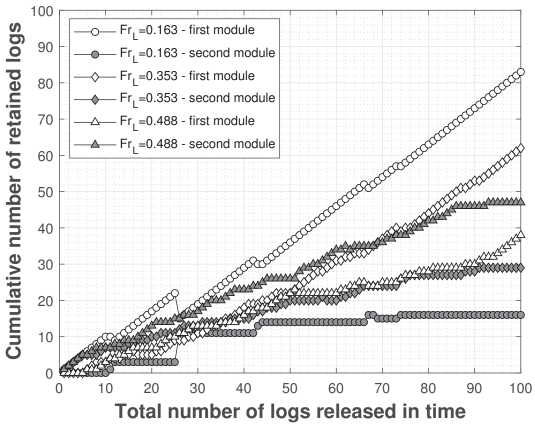

(a)

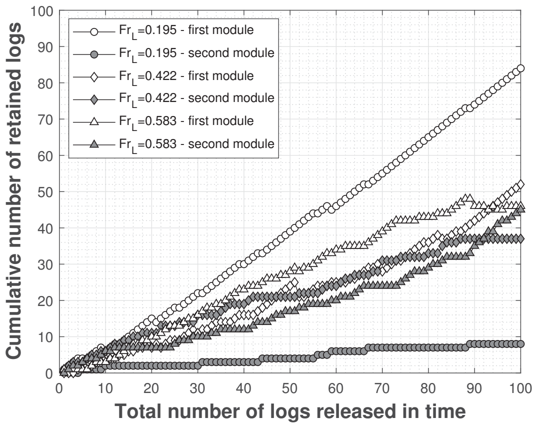

(b)

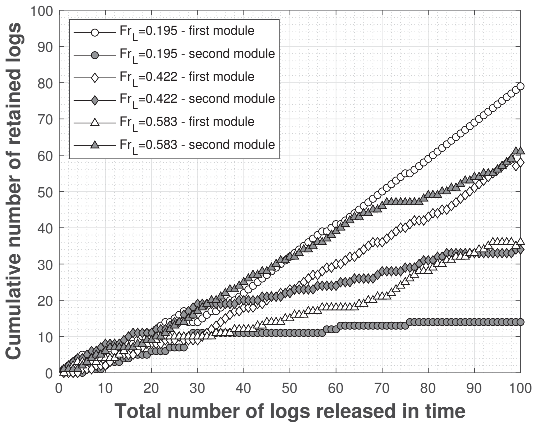

(c)

Fig. 3. Cumulative number of large wood debris trapped by individual modules of the retention system (vertical axis) versus the number of debris released in time (horizontal axis) for groups C1 (3a), C2 (3b) and C3 (3c) for three tested $\mathsf{Fr_L}$.

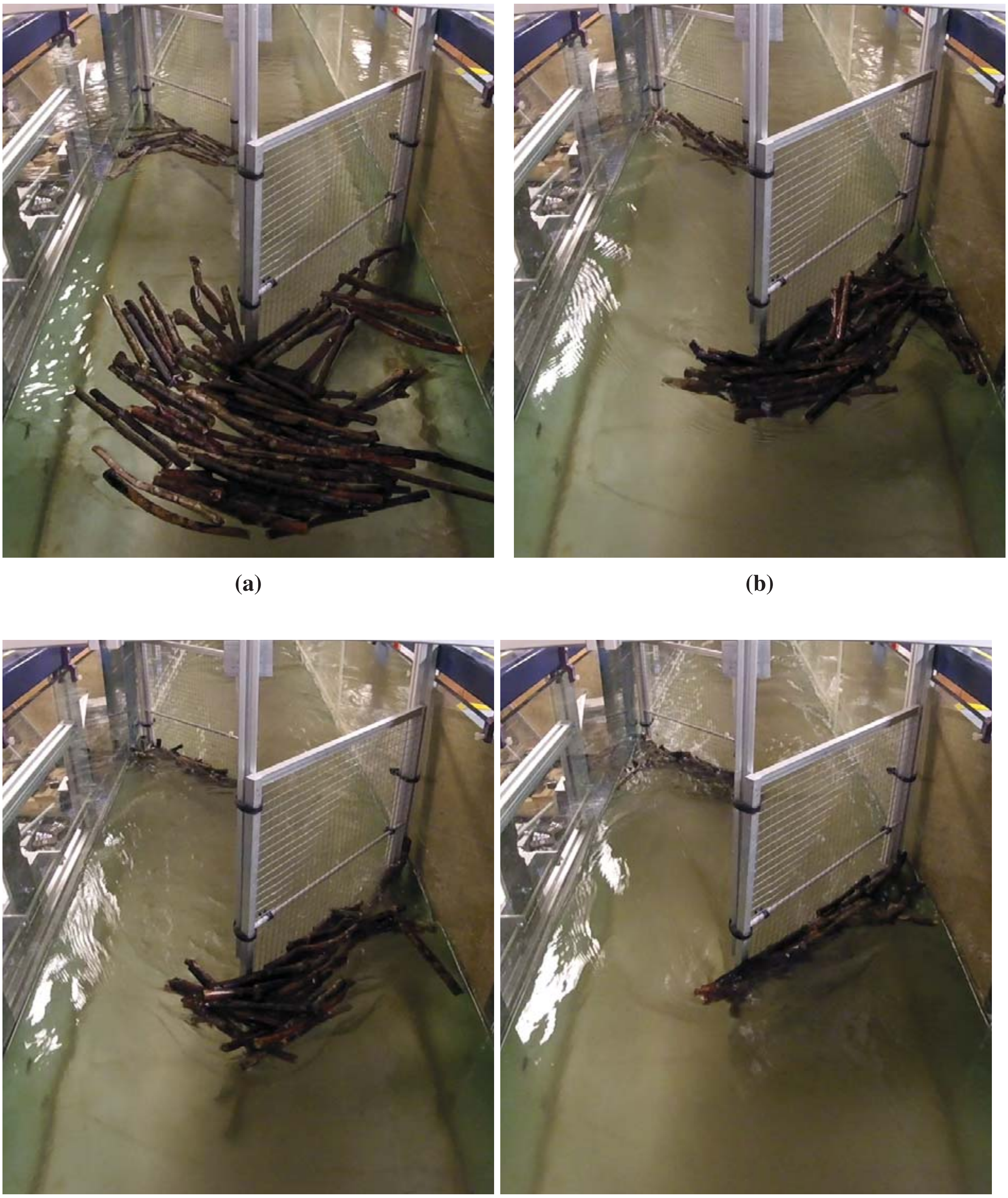

(a) (b) (c) (d)

Fig. 4. Frames from the video recordings of experimental group C2 for Fr_L=0.195 (4a), Fr_L=0.337 (4b), Fr_L=0.422 (4c) and Fr_L=0.521 (4d)

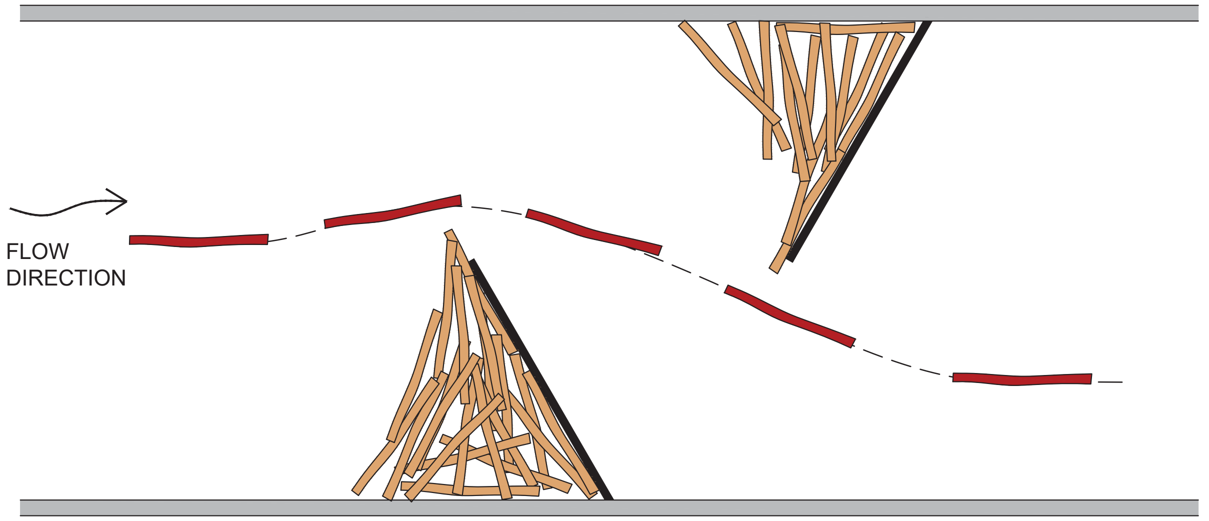

Fig. 5. Sketch of the typical trajectory followed by debris elements that passed through the retention system.

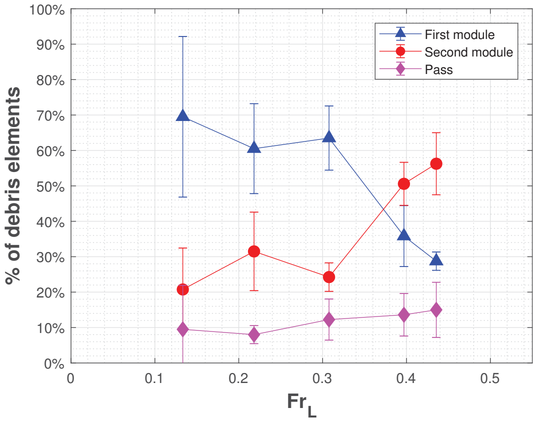

(a)

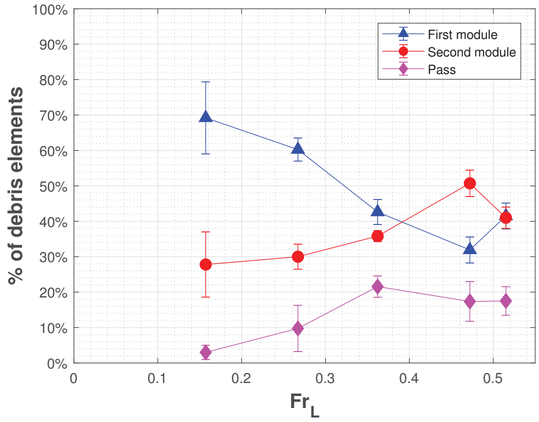

(b)

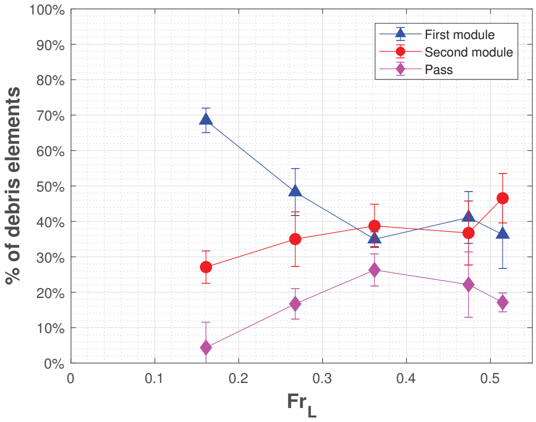

(c)

Fig. 6. Percentage of debris trapped by the first and the second modules, and the percentage of debris that passed through both modules for experimental groups B1 (6a), B2 (6b) and B3 (6c); error bars indicate a standard deviation for the four runs for each $\mathsf{Fr_L}$.

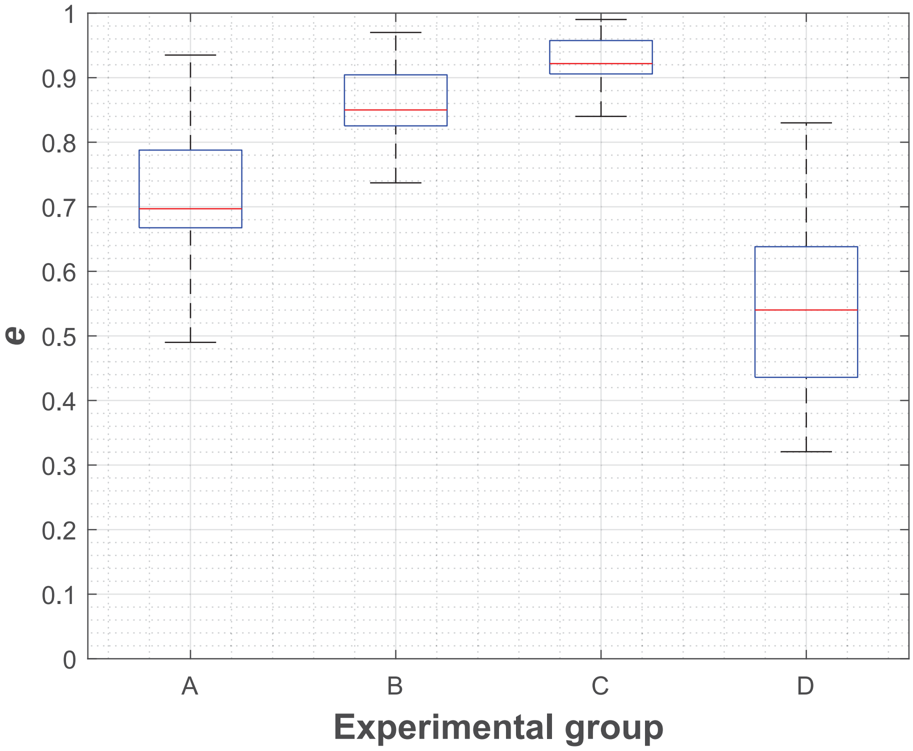

Fig. 7. Box plot of the efficiency observed for experimental groups A, B, C and D for all flow conditions and debris sizes.

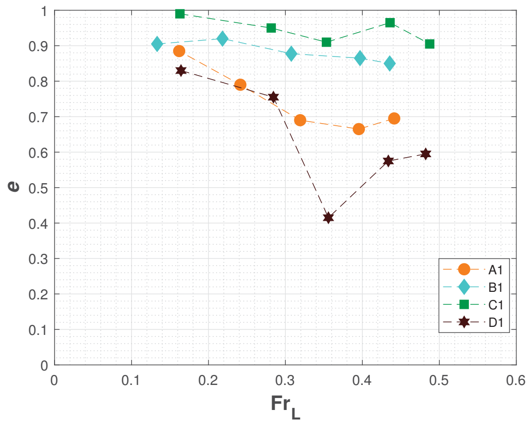

(a)

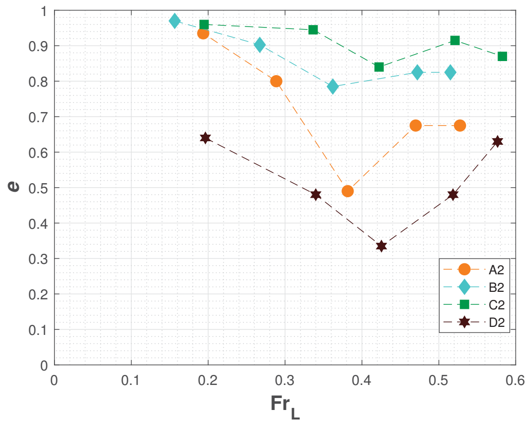

(b)

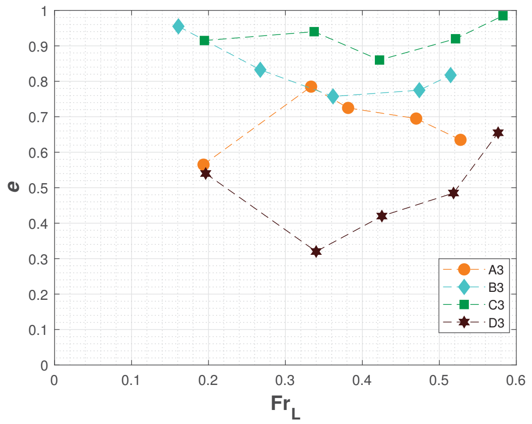

(c)

Fig. 8. Efficiency of the debris retention systems for debris length L = 250 mm, groups A1, B1, C1, and D1 (8a), L = 175 mm, groups A2, B2, C2, and D2 (8b) and mixed lengths, groups A3, B3, C3, and D3 (8c) versus $\mathsf{Fr_L}$.

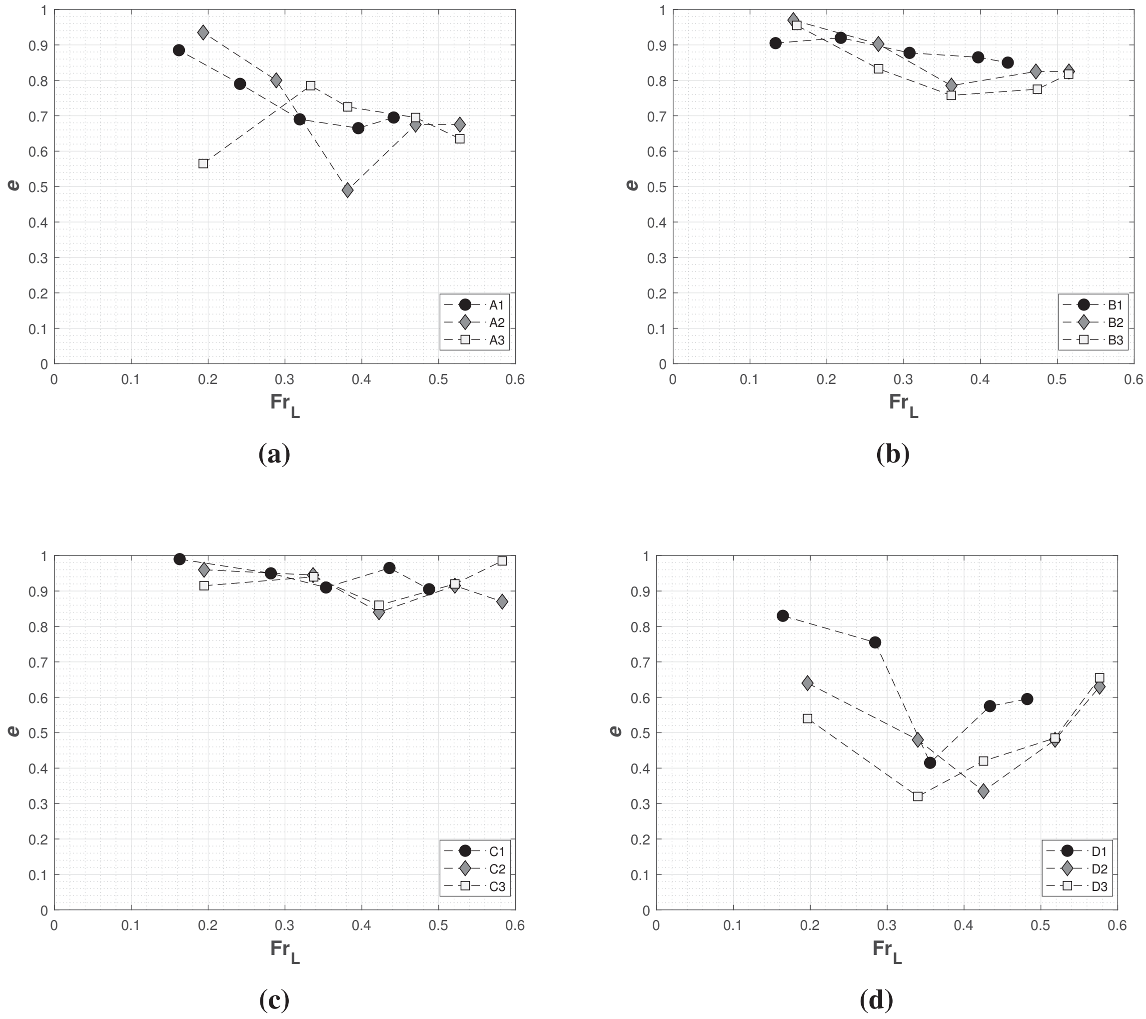

Fig. 9. Efficiency for different debris lengths at each structure, groups A1, A2 and A3 (9a), groups B1, B2 and B3 (9b), groups C1, C2 and C3 (9c) and groups D1, D2 and D3 (9d) versus $\mathsf{Fr_L}$.

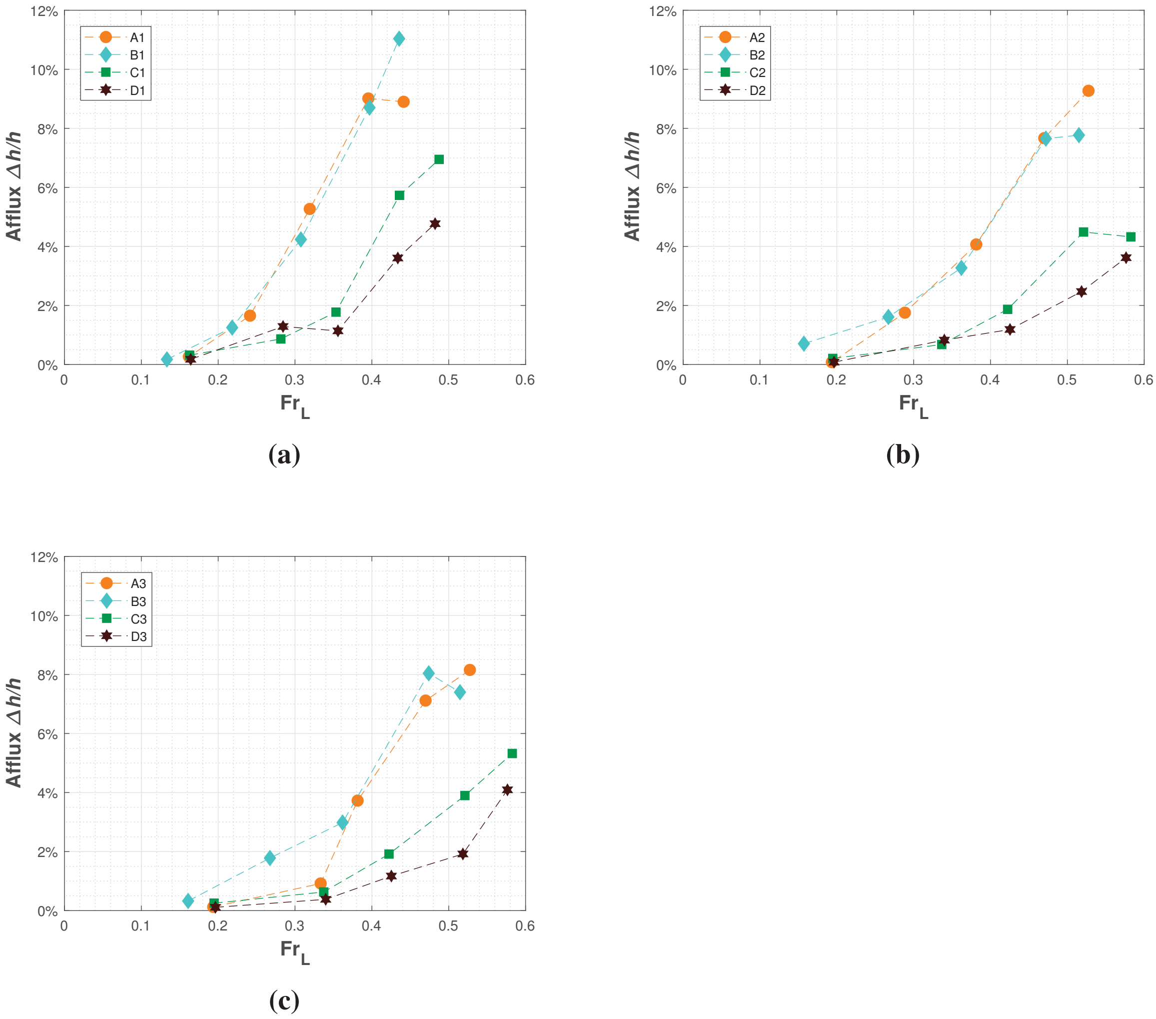

Fig. 10. Afflux (as a percentage of the undisturbed upstream flow depth) due to the accumulation of debris at the debris retention system plotted versus Fr_L for debris lengths L = 250 mm (10a) and L = 175 mm (10b) and for mixed debris (10c)

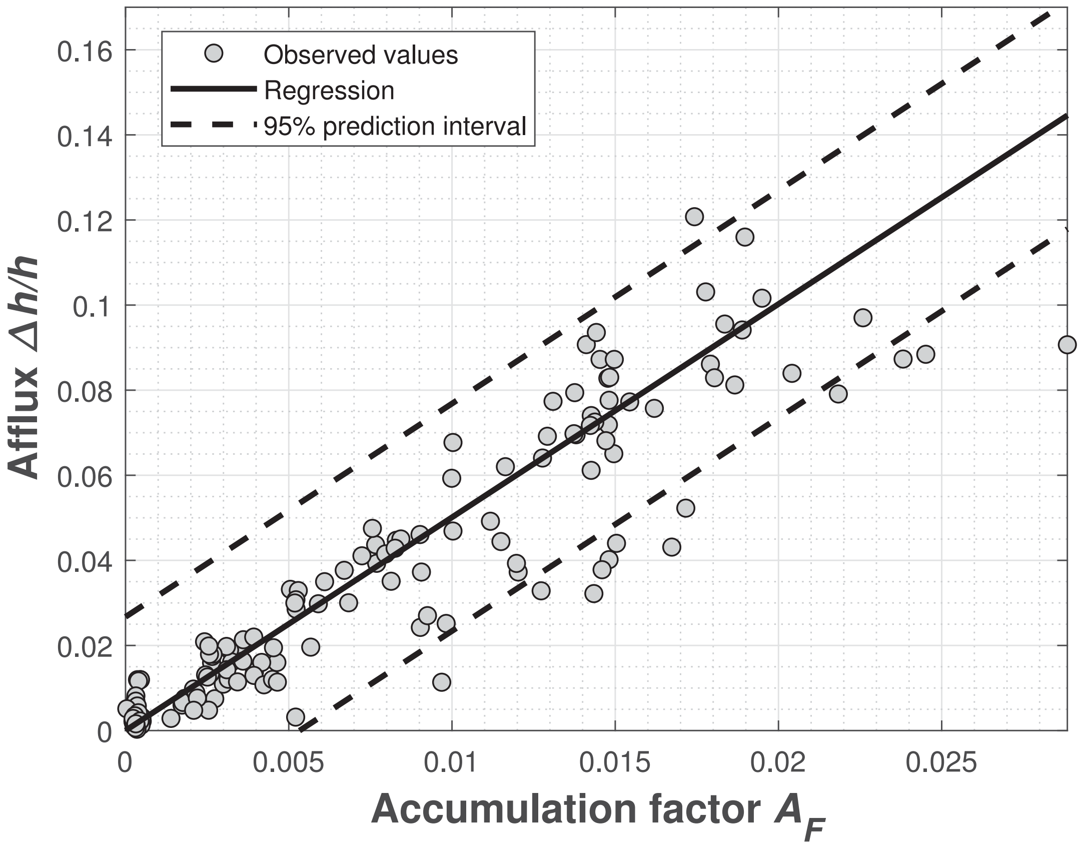

Fig. 11. Experimental data (circle points) and regression (solid line) from Equation (7) for afflux versus the accumulation factor A_F. The 95% prediction interval is also included (dashed lines).

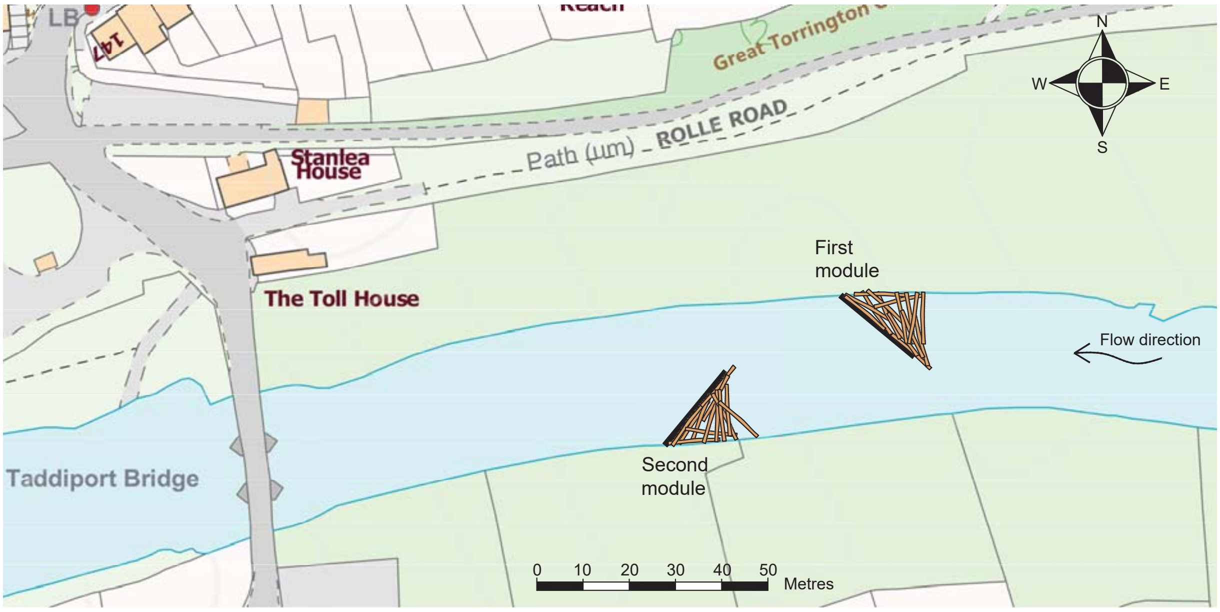

(a)

(b)

Fig. 12. Potential location for the retention system on the river Torridge between Great Torrington and Taddiport (12a) - basemap: © Crown copyright and database rights 2020 Ordnance Survey (100025252). An example of large wood debris accumulations at the nearby Taddiport Bridge (12b), photo courtesy by Devon County Council.